PHYSICAL REVIEW B VOLUME 47, NUMBER 6 1 FEBRUARY 1993-II

Structure of rings in vitreous SiO_2

José P. Rino
Universidade Federal de São Carlos (UFSCar), via Washington Lui Km. 235, Caixa Postal 676, 13560 São Carlos, São Paulo, Brazil

Ingvar Ebbsjö
The Studsvik Neutron Research Laboratory, S-611 82 Nyköping, Sweden

Rajiv K. Kalia, Aiichiro Nakano, and Priya Vashishta
Concurrent Computing Laboratory for Materials Simulations and Department of Physics and Astronomy, Louisiana State University, Baton Rouge, Louisiana 70803-4001

(Received 8 August 1991; revised manuscript received 17 September 1992)

The structure of n-fold rings in vitreous SiO_2 is investigated using molecular-dynamics configurations. A recently developed interaction potential for SiO_2 consisting of long-range Coulomb interactions, the effect of electronic polarizability, and three-body covalent forces is used in the molecular-dynamics study of the vitreous state. Results for the statistics of rings and distribution of interatomic distances and bond angles in the rings are presented for the vitreous state. The statistics of rings for the molten state is also discussed.

I. INTRODUCTION

Silicon dioxide exists in a variety of crystalline polymorphs.[1–4] The elementary unit in cristobalite[2] and quartz[3] at atmospheric pressure and in coesite[4] at high pressures is an almost ideal $Si(O_{1/2})_4$ tetrahedron. These structures are made up of different arrangements of corner-sharing tetrahedral elementary units. However, the elementary unit in stishovite,[5] which is the densest structure of SiO_2, is a distorted octahedron and the structure consists of edge- and corner-sharing octahedra.

The atomic arrangement in a crystal can be determined from diffraction experiments. From the knowledge of atomic arrangements, the nature of the elementary unit, the nearest-neighbor connectivity of the units, e.g., corner sharing or edge sharing, can be deduced. It is possible to state the nature of the connectivity of the elementary units, beyond the nearest neighbor, in terms of n-fold rings. Crystalline and disordered networks may be characterized in terms of their ring distribution by shortest-path analysis.[6] Rings defined by shortest-path analysis are a convenient way to analyze SiO_2-type covalent structures. If a silicon atom has four oxygen nearest neighbors, then there are six O-Si-O paths emanating from each Si atom. Shortest-path analysis involves taking every pair of bonds on each silicon atom in turn and finding the smallest size ring. For a fourfold-coordinated network such as a-SiO_2 at normal pressure containing N Si, atoms there are $6N$ rings. An n-fold ring therefore contains $2n$ Si-O bonds. Using this ring analysis, one finds that cristobalite consists entirely of sixfold rings, whereas quartz has sixfold and eightfold rings and coesite has fourfold, sixfold, and eightfold rings. Other crystals such as $GeSe_2$ (Refs. 7 and 8) which consist of edge- and corner-sharing tetrahedra have twofold, threefold, eightfold, and ninefold rings, whereas crystalline $SiSe_2$,[9] which consists of nonintersecting chains of tetrahedra, has only twofold rings.

Unlike crystals, atomic arrangements in glasses cannot be determined by diffraction experiments. For AX_2-type glasses, with the help of neutron- and x-ray-scattering experiments it has been possible to determine nearest-neighbor A-X, X-X, and A-A distances with a high degree of accuracy. This information, when combined with the coordination numbers, can establish the nature of the elementary unit. It has also been possible to indirectly determine the A-X-A bond angle from x-ray[10] and NMR (Ref. 11) experiments in a-SiO_2. Using this information, one can determine the connectivity of two elementary units, but the structure of n-fold rings and their distribution has not been determined experimentally in an amorphous material. Throughout this paper we have used vitreous, amorphous, and glassy states interchangeably to describe a-SiO_2.

Connectivity beyond two elementary units in a network glass has been studied using models. Models can be divided into two categories: (i) ball and stick type models as constructed by Bell and Dean[12] for a-SiO_2 and their computer-generated cousins,[13–17] and (ii) models based on atomic interaction where the evolution of the system is governed by the laws of statistical mechanics and all the approximations are contained in the choice of interparticle interaction potentials.[18–24]

Recently, an interaction potential for SiO_2 was proposed.[25] Using the molecular-dynamics (MD) method, structural correlations in amorphous and molten states are studied. The results of MD calculations compare very well with neutron-diffraction,[26] and x-ray-diffraction,[10] and NMR (Ref. 11) experiments on a-SiO_2.[25] The distribution of bond angles and the connec-

tivity of the nearest-neighbor tetrahedra were also studied using the MD configurations. It has also been possible to describe the structural modification in permanently densified a-SiO_2, and the MD results are in very good agreement with recent neutron-diffraction[27] and NMR (Ref. 28) results. The aim of this paper is to examine the distribution and structure of n-fold rings in amorphous and molten SiO_2 obtained from MD simulations.

In Sec. II we briefly describe the interaction potentials for SiO_2 and the molecule-dynamics method used in these simulations. Preparation of the amorphous state and structural correlations to characterize the nature of the amorphous state are discussed in Sec. III. In Sec. IV we discuss the statistics of n-fold rings and distributions of interatomic distances and bond angles in the rings. Conclusions are presented in Sec. V.

II. INTERACTION POTENTIALS AND MOLECULAR-DYNAMICS METHOD

A. Interaction potentials for SiO_2

Interaction potentials to study the structural and dynamical correlations in SiO_2 have recently been developed.[25] Using the molecular-dynamics technique, we have studied the structure of amorphous and molten SiO_2. These interaction potentials include two- and three-body contributions. The two-body part consists of a Coulomb interaction due to charge transfer, steric repulsion due to ionic sizes, and a charge-dipole interaction due to the large electronic polarizability of negative ions. The three-body covalent interactions include the effects of bond bending and bond stretching:

$$V=\sum_{i<j} V_2(|\mathbf{r}_{ij}|)+\sum_{i<j<k} V_3(\mathbf{r}_{ij},\mathbf{r}_{jk},\mathbf{r}_{ik}) , \tag{1}$$

where

$$V_2(r)=\frac{H_{ij}}{r^{\eta_{ij}}}+\frac{Z_iZ_j}{r}-\frac{\frac{1}{2}(\alpha_iZ_j^2+\alpha_jZ_i^2)}{r^4}e^{-r/r_{4s}} \tag{2}$$

and

$$V_3(\mathbf{r}_{ij},\mathbf{r}_{jk},\mathbf{r}_{ik})=B_{jik}f(|\mathbf{r}_{ij}|,\mathbf{r}_{ik}|)p(\theta_{jik},\bar{\theta}_{jik}) . \tag{3}$$

In the two-body interaction potential, H_{ij} and η_{ij} are strengths and exponents of the steric repulsion, Z_i and α_i are, respectively, the effective charge and electronic polarizability of the ith ion, r_{4s} is the decay length in the exponential screening term of the charge-dipole interaction, $\mathbf{r}_{ij}=\mathbf{r}_i-\mathbf{r}_j$, and θ_{jik} is the angle subtended by $\mathbf{r}_{ij}$ and $\mathbf{r}_{ki}$ at the vertex i.

Among the six three-body terms in the interaction potential in SiO_2, the most important terms involve O-Si-O and Si-O-Si because Si-O is the strongest bond in the system. The expressions for $f(r,r')$ and $p(\theta,\bar{\theta})$ in the three-body term are

$$f(r,r')=\begin{cases}\exp\left[\dfrac{1}{r-r_0}+\dfrac{1}{r'-r_0}\right] & \text{for } r,r'<r_0 ,\\ 0 \quad \text{for } r,r'\geq r_0 ,\end{cases} \tag{4}$$

$$p(\theta,\bar{\theta})=[\cos\theta-\cos\bar{\theta}]^2 . \tag{5}$$

B_{jik} is the strength of the three-body potential, $f(r,r')$ describes the bond-stretching effect, and $p(\theta,\bar{\theta})$ represents the bond-bending effects around the angle $\bar{\theta}$. For SiO_2 the values of the parameters for the interaction potential described in Eqs. (1)–(5) are given in Ref. 25.

B. Molecular-dynamics method

Using these interaction potentials, molecular-dynamics calculations were performed for a system of 648 particles (216 Si+432 O) with periodic boundary conditions. The length of the MD box was 21.392 Å, corresponding to the number density 6.62×10^{22} cm^{-3} (2.20 g/cm^3) of a-SiO_2. The equation of motion was integrated with the Beeman algorithm using a time step of 0.5×10^{-15} sec. The long-range Coulomb interaction was handled with Ewald's summation. This conserves the total energy in 1 part in 10^4 over several thousands time steps. To estimate the finite-size effects, MD calculations were also performed on a 5184-particle system.

III. PREPARATION OF THE AMORPHOUS STATE AND ITS CHARACTERIZATION USING STRUCTURAL CORRELATIONS

A. Preparation of the amorphous state

The amorphous state was obtained from a well-thermalized molten state at 2000 K. This state of SiO_2 showed small diffusion for Si and O ions. The molten state at 2000 K was quenched and thermalized to obtain a system at 1500 K. At this temperature the system shows thermal arrest and long-range diffusion shows a marked decrease. However, local rearrangements continue to take place because of the considerable thermal energy that is available to particles. From the well-thermalized 1500-K system, 600- and 310-K systems were obtained by subsequent cooling and thermalizing. A detailed description of the quenching and thermalization schedules is given in Ref. 25. Analysis of rings was carried out on the amorphous state at 310 K and the molten state at 2500 K.

B. Characterization of the amorphous state

Before discussing the analysis of a system in terms of n-fold rings, it may be useful to briefly look at a few important structural correlations in the amorphous state. In Fig. 1 we examine the calculated neutron structure factor for the amorphous state and compare it with experimental results to establish the quality of our MD simulations. All the peaks including the first sharp diffraction peak in the MD results are in good agreement with neutron experiments.[26] The partial pair distribution function $g_{\alpha\beta}(r)$ for Si-Si, Si-O, and O-O is shown in Fig. 2. Calculated bond lengths and full width at half maximum (FWHM) for Si-Si, Si-O, and O-O are, respectively, 3.10 Å (0.20 Å), 1.62 Å (0.05 Å), and 2.64 Å (0.15 Å), in good agreement with corresponding experimental results, 3.08, 1.61, and 2.63 Å, by Johnson, Wright, and Sin-

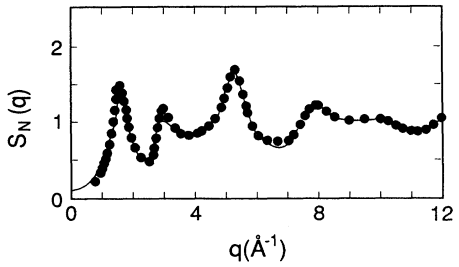

FIG. 1. Neutron static structure factor for a-SiO_2. The solid curve is the MD calculation, and the solid circles are from neutron-diffraction experiments (Ref. 26).

clair.[26] From the area under the first peak in $g_{Si\text{-}O}(r)$, the Si-O coordination is found to be 4. This suggests that the elementary unit is a tetrahedron. To further examine the nature of the elementary unit, the total bond-angle distributions for O-Si-O, O-O-Si, O-O-O, Si-Si-Si, Si-Si-O, and Si-O-Si are shown in Figs. 3(a) and 3(b). The O-Si-O distribution peaks at 109° with a FWHM of 10°, in agreement with experiments.[29] The O-O-Si and O-O-O distributions peak at 35° and 60°, respectively. For a perfect tetrahedron, the corresponding angles are 35.3° and 60°, respectively. The Si-O-Si distribution has been inferred from NMR experiments. The peak in the calculated distribution is at 142° with a FWHM of 25°, in agreement with the corresponding experimental value of 142° with a FWHM of 26°.[11] From partial pair distribution functions and total bond-angle distributions, we infer that in a-SiO_2 the elementary unit is on the average a nearly perfect tetrahedron.

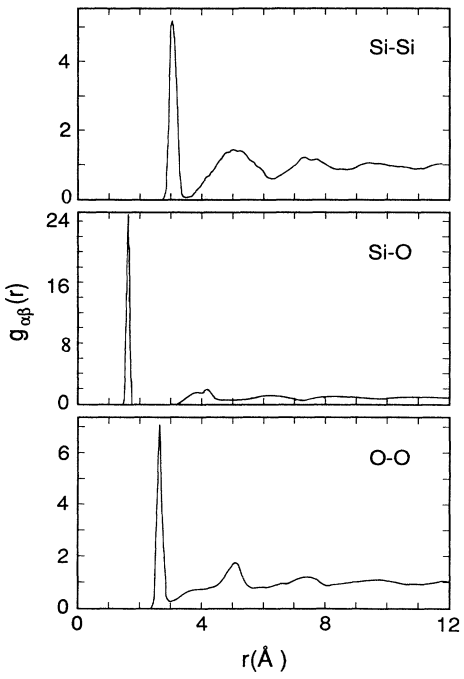

FIG. 2. Partial pair distribution functions for Si-Si, Si-O, and O-O in a-SiO_2 at 310 K.

IV. STRUCTURE OF n-FOLD RINGS

Analysis of rings is done in three steps. We first investigate the statistics of n-fold rings of sizes $n=2$–11, and then the distributions of interatomic distances and bond angles are calculated within each ring and averaged over all rings of the same size.

A. Statistics of rings in a-SiO_2

The connectivity of a covalent network can be described in terms of n-fold rings. The distribution of n-

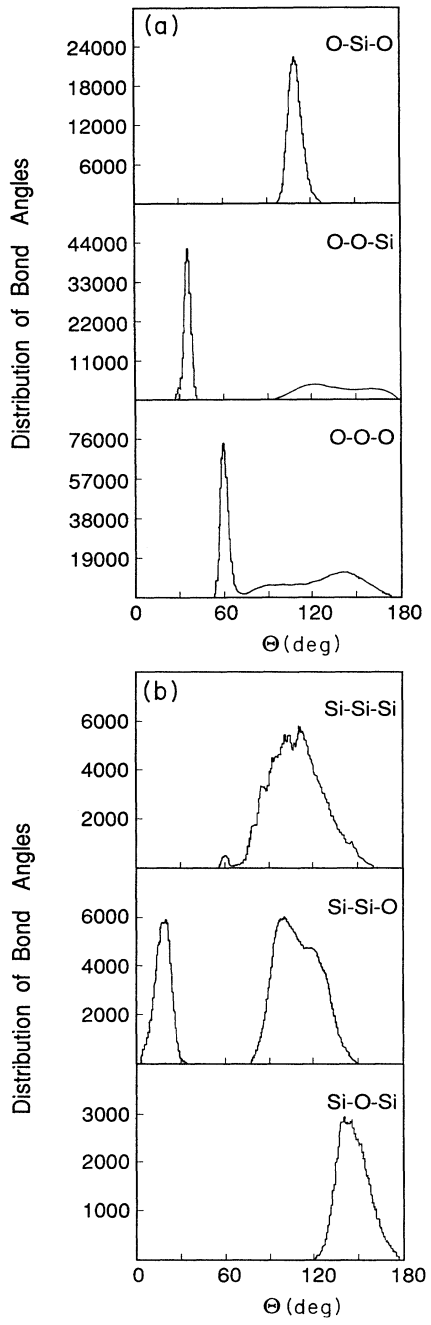

FIG. 3. Bond-angle distributions for a-SiO_2 at 310 K.

fold rings is determined in the following manner: First of all, one constructs a list of nearest neighbors (NN's) for each Si and O in the system (there are on the average four NN O around a Si and two Si around an O). Let O_1, O_2, O_3, and O_4 be the NN's of Si_1. There are six paths of the type O_1-Si_1-O_2 starting from Si_1. To determine the shortest closed path starting from O_1-Si_1-O_2, one finds the NN Si atom of O_2, Si_2, and continues this process until one returns to O_1. Such an n-fold ring contains $2n$ Si-O bonds. For N Si atoms in the system, there are on the average $6N$ rings. The statistics of n-fold rings is calculated for a-SiO_2 using 100 molecular-dynamics configurations. For comparison, the statistics of rings was also calculated for α- and β-cristobalite and α- and β-quartz. The results for the statistics of n-fold rings per Si tetrahedron are summarized in Table I.

From Table I one observes that (i) there are no twofold rings (edge-sharing tetrahedra) in a-SiO_2, (ii) the number of threefold rings is very small, 1% of the total number of rings, (iii) the distribution is peaked at sixfold rings and it is nearly symmetric around $n=6$, and (iv) the total number of rings per tetrahedron is 5.74 instead of 6. This small discrepancy is due in part to the cutoff in the Si-O distance used in determining the list of nearest neighbors and the finite size of the MD box, which limits the size of the largest ring admissible in the system.

B. Interatomic distances and bond angle distributions in n-fold rings

The following facts, which have been established from the pair distribution functions and total bond-angle distributions, should be kept in mind while examining the structure of n-fold rings: (i) The Si-O bond and O-Si-O tetrahedral angle are very robust, and (ii) the Si-O-Si angle is flexible, but to only within about 25° of the mean value of 142°.

1. Twofold rings

Edge-sharing tetrahedra or twofold rings are not found in a-SiO_2. One of the following two possibilities must happen in order to form an edge-sharing tetrahedron. The first is that the O-Si-O and Si-O-Si angles are nearly 90°, and the second is that the O-Si-O angle is close to the tetrahedral angle 109° and the Si-O-Si angle is around 70°. Both of these possibilities are energetically very unfavorable, and there is no evidence of large angular distortions, needed for an edge-sharing configuration, in any of the crystalline structures of SiO_2.

2. Threefold rings

The formation of a threefold ring requires less distortion when compared to an edge-sharing tetrahedra. However, the distortion required in the Si-O-Si angle is still substantial and only 1% of the total rings are threefold rings. Figures 4(a) and 4(b) show, respectively, the distribution of interatomic distances and bond angles in threefold rings. This ring size is characterized by well-defined Si-Si, O-O, and Si-O distances. From Fig. 4(b) the peak position of the O-Si-O angle distribution is at 102° and it is about 35° for O-O-Si, implying that the tetrahedra in threefold rings are very distorted. Both the Si-Si-Si and O-O-O bond angle distributions are peaked at 60°, suggesting that the threefold ring has one plane containing three Si and the other plane containing three O atoms. The Si-O-Si bond-angle distribution is asymmetric and peaked around 130°. It shows the largest distortion from the peak at 142° in the total Si-O-Si bond-angle distribution. In addition, there are two environments for threefold rings: one corresponding to the Si-O-Si angle of 120° and the other to the Si-O-Si angle of 132°.

Using the bond-length and -angle data for threefold rings, $r_{\text{Si-O}}=1.62$ Å, $\theta_{\text{O-Si-O}}=102°$, $\theta_{\text{Si-O-Si}}=132°$, $\theta_{\text{O-O-O}}=60°$, and $\theta_{\text{Si-Si-Si}}=60°$, we can determine the nonplanarity of threefold rings. $\theta_{\text{O-O-O}}=60°$ and $\theta_{\text{Si-Si-Si}}=60°$ imply that Si and O form equilateral triangles. Using a simple model where the two triangles are separated by a distance h and are rotated with respect to each other by 60°, the distance h can be calculated using the bond-length and -angle information given above. First, we can estimate

$$r_{\text{Si-Si}}=2r_{\text{Si-O}}\sin(\theta_{\text{Si-O-Si}}/2)=2.96\text{Å}$$

and

$$r_{\text{O-O}}=2r_{\text{Si-O}}\sin(\theta_{\text{O-Si-O}}/2)=2.52\text{Å}\ ,$$

which are consistent with the MD data [see Fig. 4(a)]. Using this information, one can also determine the Si-O distance. By comparing it with the given value 1.62 Å, we can determine the height, $h=0.27$ Å, separating the Si-Si-Si and O-O-O triangles. The other peaks in the bond-length and -angle data [Figs. 4(a) and 4(b)] are consistent with this model. This analysis, therefore, establishes that even the threefold rings are not planar.

No evidence of an adamantanelike cage consisting of four identical puckered threefold rings has been found.[30] Threefold rings are most frequently found as members of larger rings ($n\geq 5$). We comment on this feature when the O-O-O angle distribution is discussed for larger rings.

3. Fourfold rings

The distributions of interatomic distances and bond angles for $n=4$ are shown in Figs. 5(a) and 5(b). The Si-O and O-O bond lengths correspond to a nearly undistorted

TABLE I. Statistics of n-fold rings per $Si(O_{1/2})_4$ tetrahedron in a-SiO_2 at 310 K.

Ring size (n)	2	3	4	5	6	7	8	9	10	11
α- and β-cristobalite					6					
α- and β-quartz					4		2			
a-SiO_2		0.06	0.52	1.40	2.11	1.18	0.40	0.06	0.01	

tetrahedron. From Fig. 5(b), the O-Si-O angle is found to be 106°, implying a 3° distortion in the tetrahedral angle, and the O-O-Si angle is nearly 40°. The O-O-O angle has a peak at 90° with a FWHM of 20°, suggesting a roughly square arrangement of O atoms. The Si-Si-Si distribution shows a three-peak structure with the main peak at 85° and two other peaks at 77° and 60°. Clearly, the fourfold ring consisting of four Si and four O is not a planar ring. The peak position of FWHM of the Si-O-Si distribution in fourfold rings looks similar to the Si-O-Si total angle distribution [Fig. 3(b)].

4. Fivefold and larger rings

Distributions of interatomic distances and bond angles for $n \geq 5$ are shown in Figs. 6–10, including the distributions in the most common rings ($n = 5$, 6, and 7). In these larger rings, the peak positions in O-Si-O bond-angle distributions are very close to 109°, indicating that the larger rings consist of nearly perfect tetrahedra. Also, the O-Si-O distributions in larger rings are similar to the total distribution. We can see that the tetrahedra in larger rings are less distorted than those in smaller

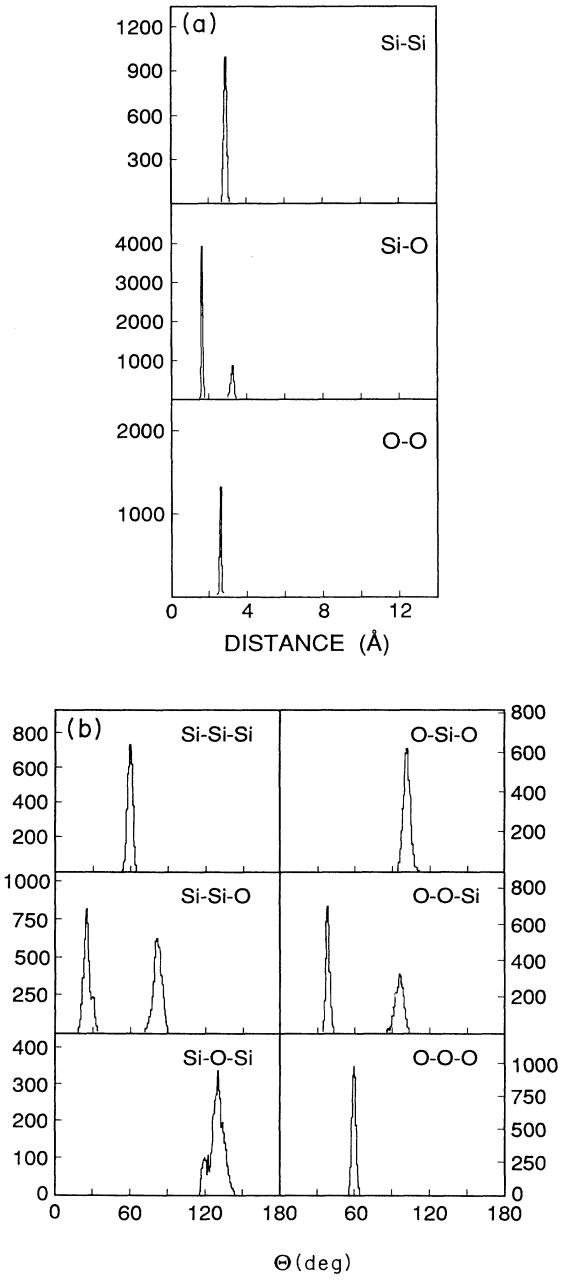

FIG. 4. (a) Interatomic distance distributions and (b) bond-angle distributions in threefold rings.

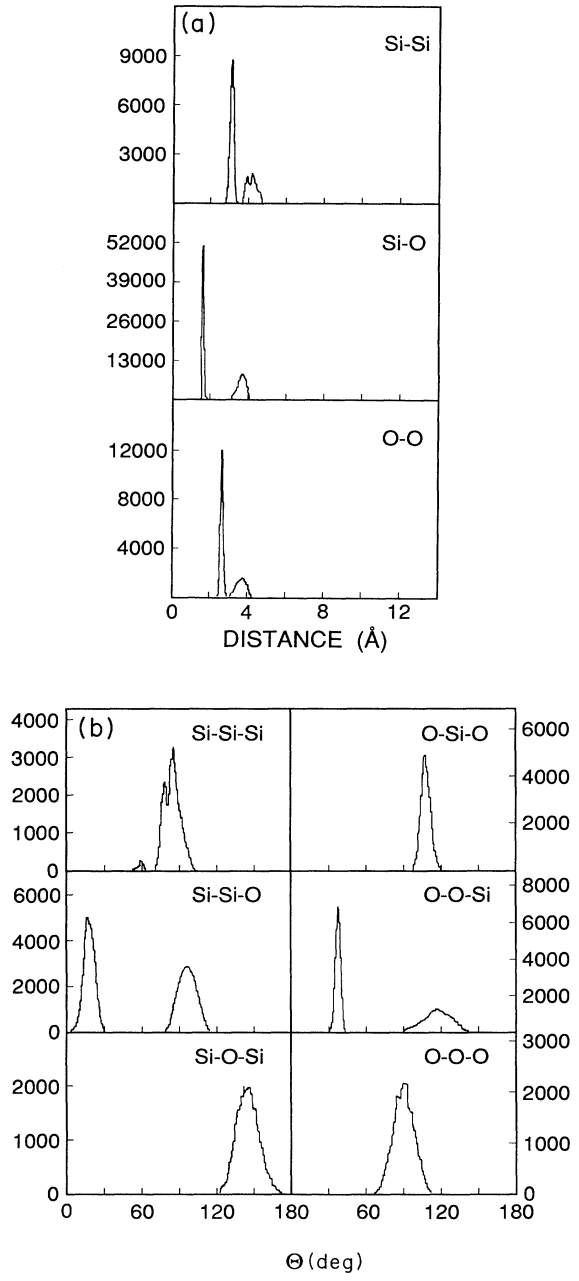

FIG. 5. (a) Interatomic distance distributions and (b) bond-angle distributions in fourfold rings.

rings. One remarkable feature in these distributions is that the O-O-O bond-angle distribution for larger rings, $n \geq 5$, has a bump at 60° in addition to a broad peak at larger angle. The bump is reminiscent of the peak at 60° of the O-O-O bond-angle distribution in threefold rings. The bump arises from configurations in which threefold rings share atoms with larger rings. The threefold rings in the shared configurations cause the distortion in the larger rings which is manifested as a small bump in the O-O-O distributions at 60°. Furthermore, this 60° bump in the O-O-O distributions in larger rings supports our analysis of the double-peak structure in the Si-O-Si distribution for threefold rings [Fig. 4(b)] as showing two environments for threefold rings.

Another point to be noted is that the Si-O-Si bond-angle distribution for fivefold rings has an asymmetric peak. An asymmetric peak in the Si-O-Si distribution is also observed for threefold rings. In fourfold and sixfold rings, the peak is much more symmetric. The difference in the peak shapes implies the difference in ordering between odd and even rings.

C. Planar rings in a-SiO_2

Planar rings have been postulated in an effort to understand Raman spectra of a-SiO_2. Based on an energy-

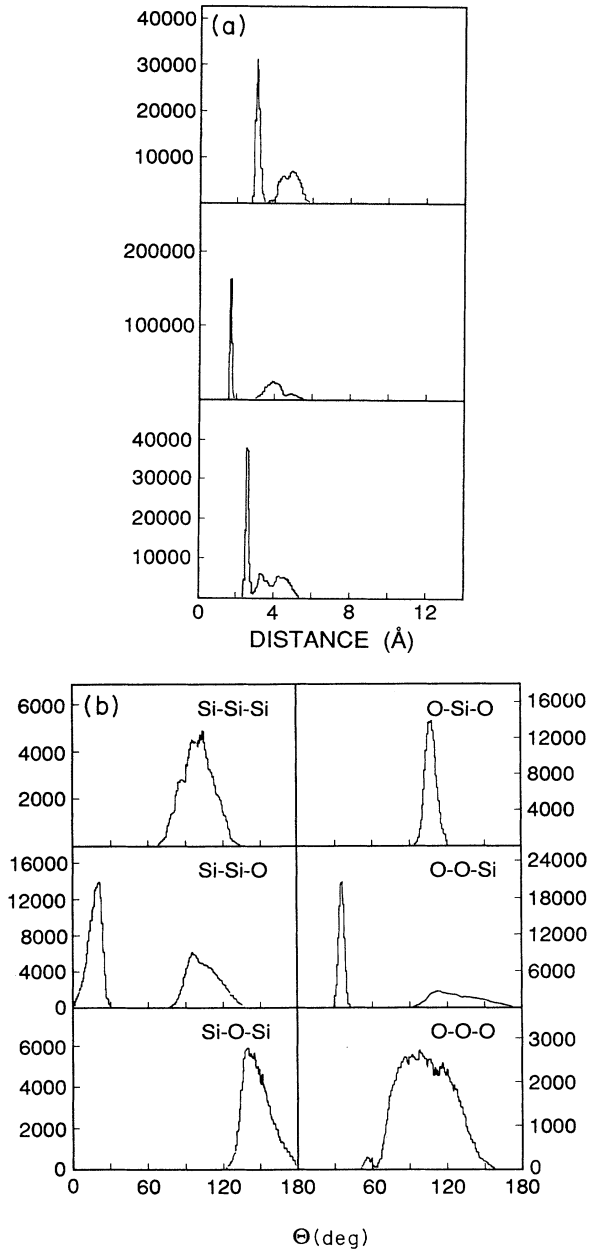

FIG. 6. (a) Interatomic distance distributions and (b) bond-angle distributions in fivefold rings.

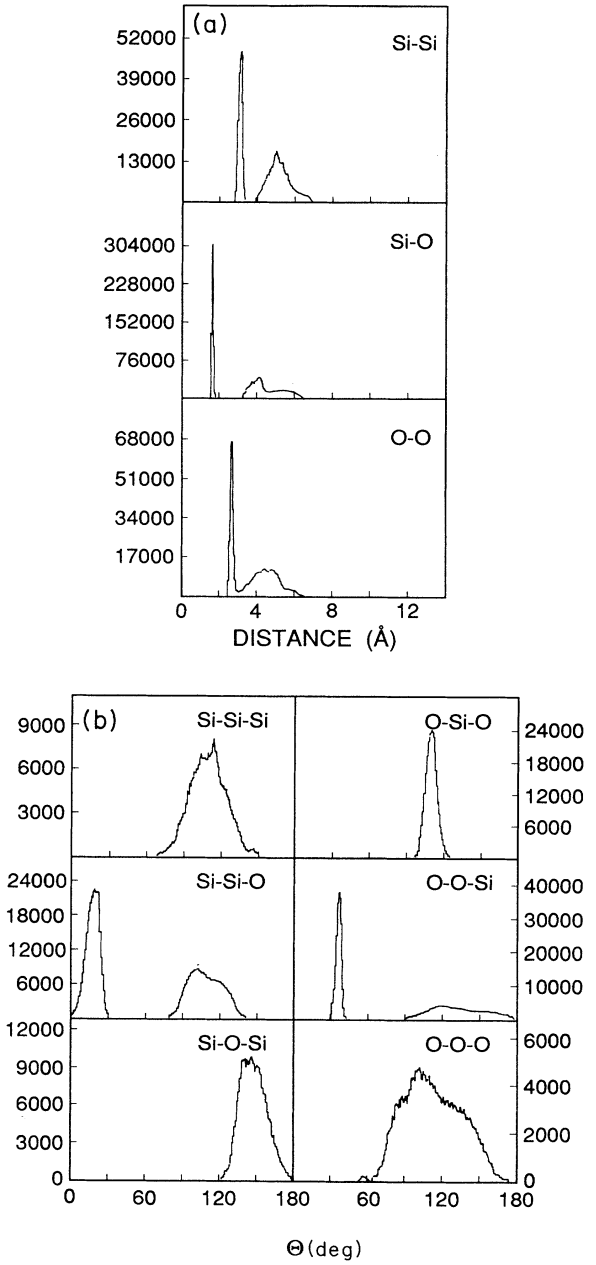

FIG. 7. (a) Interatomic distance distributions and (b) bond-angle distributions in sixfold rings.

minimization argument, Galeener proposed that planar rings exist in a-SiO_2.[30] He assigned the sharp D_2 line at 606 cm^{-1} observed in Raman spectra to a symmetric stretch mode of a planar threefold ring. The relation between the O-Si-O angle, denoted by ϕ, and the Si-O-Si angle, denoted by θ, for an n-fold planar ring is given by the relation

$$\theta \equiv \Theta_n(\phi) = 360\left[1-\frac{1}{n}\right]-\phi \ . \tag{6}$$

Figure 11 shows regular planar n-fold rings for $n=3-7$, subject to the constraint that ϕ is the perfect tetrahedral angle, $\phi_0 = 109.5°$. The value of $\Theta_n(\phi_0)$ for $n=3-12$ is given in column 3 of Table II. It is clear from the figure and column 3 of Table II that for $n>5$ the Si-O-Si angle $\Theta_n(\phi_0)$ is greater than 180°; i.e., the rings are involuted.

Using molecular-dynamics configurations, the structure of rings has been investigated in Sec. II B. Twofold rings are not found in a-SiO_2. For $n=3-10$, the values of the Si-O-Si and O-Si-O angles denoted by ϕ_{MD} and θ_{MD} are given in the columns 4 and 6 of Table II, respectively. To take into account the distortion of the O-Si-O angle from its tetrahedral value, ϕ_{MD} in column 4 is used to evaluate $\Theta_n(\phi_{MD})$ using Eq. (6). The results are given

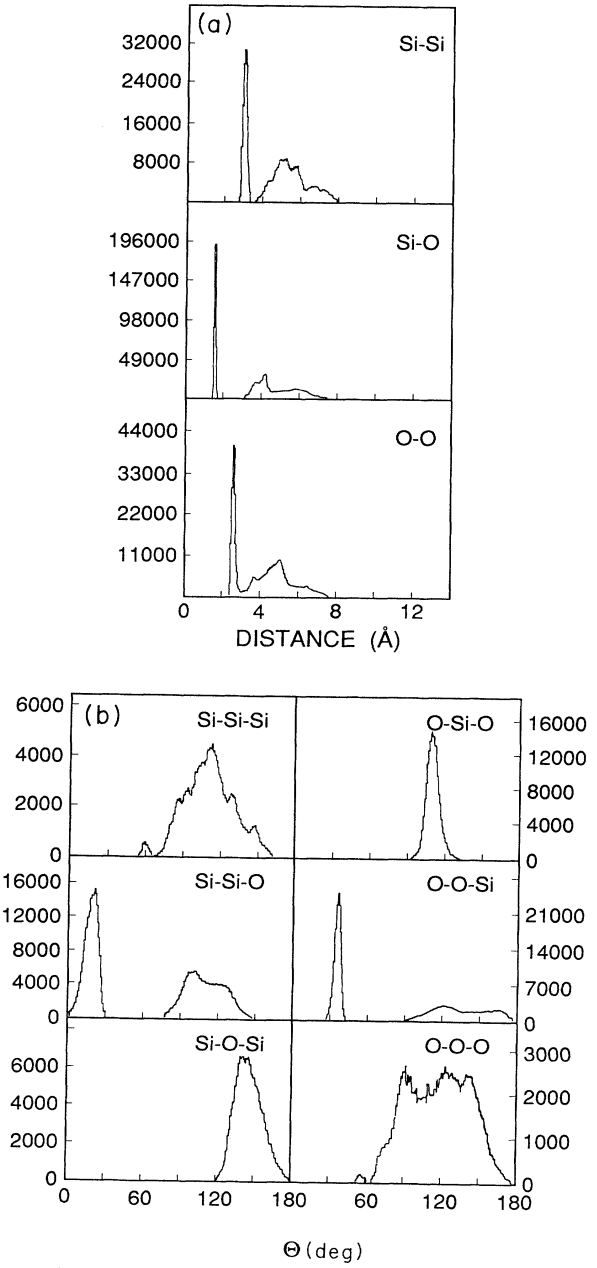

FIG. 8. (a) Interatomic distance distributions and (b) bond-angle distributions in sevenfold rings.

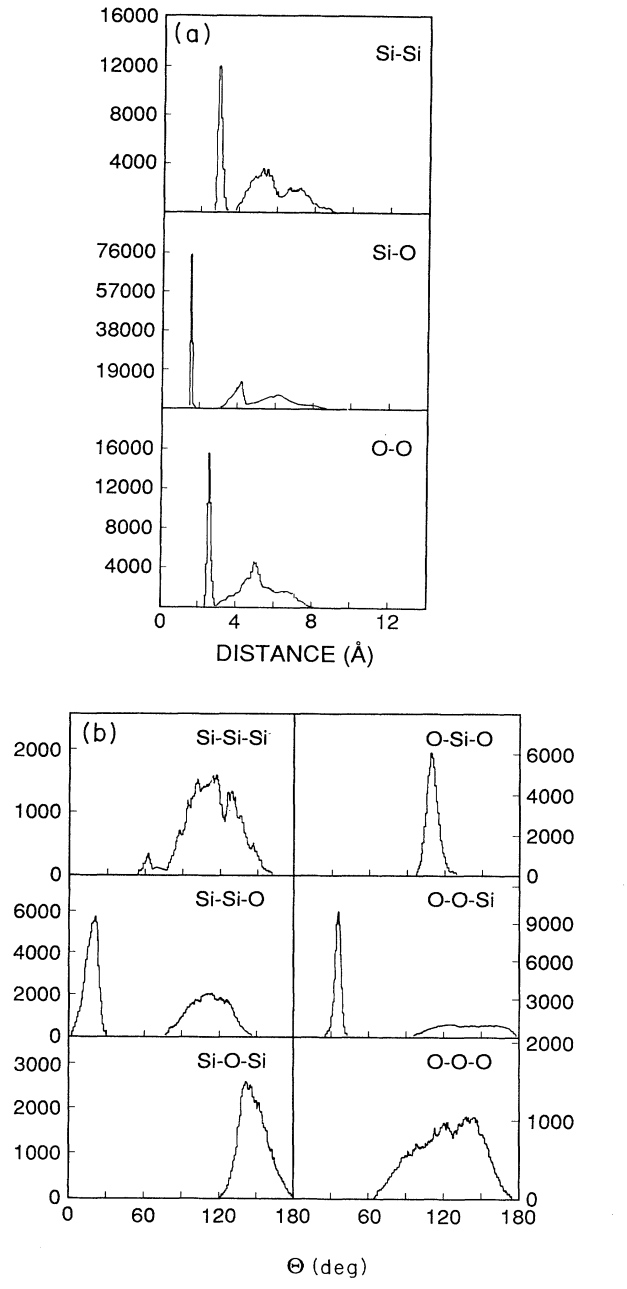

FIG. 9. (a) Interatomic distance distributions and (b) bond-angle distributions in eightfold rings.

TABLE II. Bond angles in n-fold rings. In column 3, the Si-O-Si angle $[\Theta_n(\phi_0)]$ in a regular planar n-fold ring is calculated from Eq. (6) with the O-Si-O angle ($\phi_0 = 109.5°$). Results from MD simulations are given in columns 4 and 6 for ϕ_{MD} and θ_{MD}, the O-Si-O and Si-O-Si angles, respectively, averaged over n-fold rings. θ in column 5 $[\Theta_n(\phi_{MD})]$ is calculated from Eq. (6) using $\phi = \phi_{MD}$ from column 4. Populations of n-fold rings in MD configurations are given in the last column.

	Planar rings		Molecular-dynamics simulations of a-SiO_2 at 310 K			
n	ϕ_0	$\Theta_n(\phi_0)$	ϕ_{MD}	$\Theta_n(\phi_{MD})$	θ_{MD}	Population
3	109.5	130.5	102.0	138.0	130.5	1,197
4	109.5	160.5	106.0	164.0	145.0	11,282
5	109.5	178.5	108.0	180.0	140.0	30,209
6	109.5	190.5	108.5	191.5	144.5	45,536
7	109.5	199.1	109.5	199.1	142.0	25,440
8	109.5	205.5	109.5	205.5	142.0	8,407
9	109.5	210.5	109.0	211.0	146.0	1,376
10	109.5	214.5	109.5	214.5	144.0	111
11	109.5	217.8				
12	109.5	220.5				

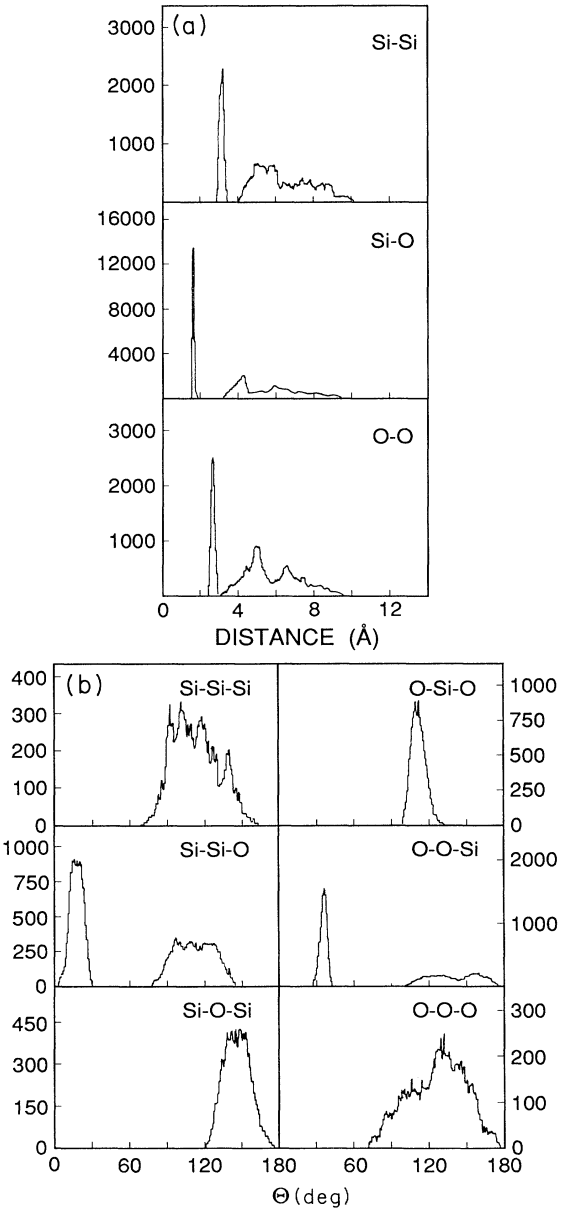

FIG. 10. (a) Interatomic distance distributions and (b) bond-angle distributions in ninefold rings.

in column 5 of Table II. By comparing the results given in columns 5 and 6, it is clear that the description of planar rings which include the distortion of the tetrahedral angle is in disagreement with the results of MD simulations. The population of rings is given in the last column of Table II. When ϕ_{MD} and θ_{MD} are weighted with the population of n-fold rings, the average values are $\langle \phi_{MD} \rangle = 108.4°$ and $\langle \theta_{MD} \rangle = 142.6°$. These values are consistent with the position of the peaks in the total bond-angle distributions given in Figs. 3(a) and 3(b).

Analysis of threefold rings when combined with the above discussion results in the conclusion that there are no planar rings in a-Si-O_2.

D. Energetics of n-fold rings in a-SiO_2

A qualitative understanding of the energetics of rings in a-SiO_2 can be achieved by examining the interatomic distance and bond-angle distributions in n-fold rings.

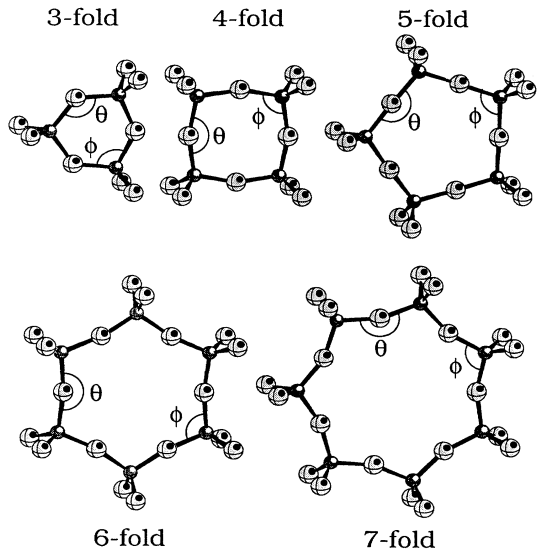

FIG. 11. Regular planar n-fold rings for $n = 3$–7. Small and large spheres represent Si and O atoms, respectively. ϕ and θ denote O-Si-O and Si-O-Si bond angles. Using the perfect tetrahedral angle 109.5° for ϕ, θ is determined from Eq. (6).

With respect to the crystalline phase, there are three important energy scales in the system. Since Si-O is the strong cohesive bond, the two most important bond angles involving this bond are the internal tetrahedral angle O-Si-O and the angle between two tetrahedra, Si-O-Si. Therefore an energy function should contain at least the following three terms: (i) energy to stretch the Si-O bond from its mean value, (ii) energy to bend the O-Si-O bond from its mean value, which is usually very close to the tetrahedral angle of 109°, and (iii) the bending energy of the Si-O-Si bond away from its average value. We call such a function ΔE_n, which can be written as

$$\Delta E_n = E_0 \left[\frac{A_r}{\sigma_r^2}(r-\langle r\rangle)^2 + \frac{A_\phi}{\sigma_\phi^2}(\phi-\langle\phi\rangle)^2 + \frac{A_\theta}{\sigma_\theta^2}(\theta-\langle\theta\rangle)^2 \right], \quad (7)$$

where σ_r, σ_ϕ, and σ_θ are the FWHM of the Si-O bond-length distribution and the O-Si-O and Si-O-Si bond-angle distributions, respectively. $\langle r\rangle$, $\langle\phi\rangle$, and $\langle\theta\rangle$ are the mean values of the Si-O bond length and the O-Si-O and Si-O-Si bond angles, respectively. A_r, A_ϕ, and A_θ are the constants which represent relative weights of the three terms, and E_0 can be thought of as an energy scale related to the cohesive energy of the material.

To examine the energetics of rings as a function of n, we have for now left out the effect of the Si-O bond stretching, $A_r=0$. Taking $\sigma_\phi=10°$, $\sigma_\theta=25°$, $\langle\phi\rangle=108.4°$, and $\langle\theta\rangle=142.6°$, with $A_\theta=1$ and $A_\phi=1$, we have plotted the function $\varepsilon(n)=\Delta E_n/E_0$ and the relative population of the rings, $P(n)$, as functions of ring size n. The results are shown in Fig. 12. It is clear from the figure that threefold rings are energetically the most unfavorable. This is consistent with the fact that only 1% of the total rings are threefold rings. There is a shallow energy minimum at $n=6$ and a corresponding maxima in the population of rings.

The effect of including the first term due to Si-O bond stretching in the energy function [Eq. (7)] will be to increase further the energy of threefold rings. This is mainly because the Si-O bond suffers its largest distortion from the average value in threefold rings.

E. Statistics of n-fold rings in molten SiO_2

The statistics of rings in molten SiO_2 at 2500 K is given in Table III. It is noteworthy that even though the liquid

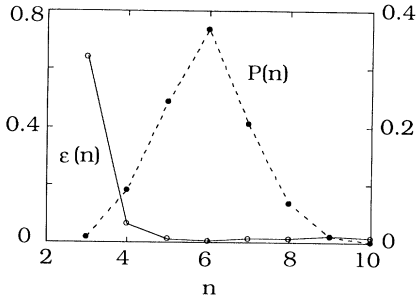

FIG. 12. Energy function (open circles) $\varepsilon(n)=\Delta E_n$ [see Eq. (7)] and relative populations (solid circles) $P(n)$ of n-fold rings in a-SiO_2.

allows much more distortion of the local environment, no twofold rings are found in the system. The populations of threefold and fourfold rings decrease in molten SiO_2 when compared to the respective populations in a-SiO_2 at 310 K. The population of the threefold rings decreases to 0.04 from 0.06 and of the fourfold rings to 0.44 from 0.52. Conversely, the populations of eightfold, ninefold, and tenfold rings increase somewhat in the melt.

V. CONCLUSION

We have examined the statistics of n-fold rings in amorphous and molten SiO_2. The structure of rings for $n=3-10$ is studied by examining the interatomic distance and bond-angle distributions within rings. No edge-sharing tetrahedra are found in a-SiO_2 at 310 K or in the molten system at 2500 K. The population of threefold rings is about 1% of the total number of rings. The energetics of rings suggest a very high energy for threefold rings. No planar rings are found and the population of threefold and fourfold rings decreases in the molten phase. Clearly, an unsophisticated analysis of the structure and vibrational spectra of a-SiO_2 based on planar rings[30] is not suitable for real material.

In the process of examining the phonon density of states in a-SiO_2, we plan to analyze the eigenvectors for rings of various sizes. It remains to be seen whether a well-defined frequency mode can be assigned to a particular ring in a-SiO_2.

TABLE III. Statistics of n-fold rings per $Si(O_{1/2})_4$ tetrahedron in molten SiO_2 at 2500 K.

Ring size (n)	2	3	4	5	6	7	8	9	10	11
Molten SiO_2		0.04	0.44	1.31	2.00	0.98	0.69	0.24	0.04	

ACKNOWLEDGMENTS

We would like to thank Dr. Sherman Susman, Dr. David Price, Dr. Marcos Grimsditch, and Dr. Adrian Wright for many helpful discussions. This research is supported in part by Louisiana Education Quality Support Fund, Grant No. LEQSF-(1991-92)-RD-A-05, and U.S. DOE, Grant No. DE-FG05-92ER45477.

[1]F. Liebau, in *The Physics and Technology of Amorphous SiO_2*, edited by R. A. B. Devine (Plenum, New York, 1988), p. 15.
[2]J. J. Pluth, J. V. Smith, and J. Faber, Jr., J. Appl. Phys. **57**, 1045 (1985).
[3]L. Levien, C. T. Prewitt, and D. J. Weidner, Am. Mineral. **65**, 920 (1980).
[4]L. Levien and C. T. Prewitt, Am. Mineral. **66**, 324 (1981).
[5]L. L. Liu, W. A. Bassett, and T. Takahashi, J. Geol. Res. **79**, 1160 (1974).
[6]A. C. Wright and J. A. E. Desa, Phys. Chem. Glasses **19**, 140 (1978).
[7]Von G. Dittmar and H. Schäfer, Acta Crystallogr. B **32**, 2726 (1976).
[8]P. Vashishta, R. K. Kalia, G. A. Antonio, and I. Ebbsjö, Phys. Rev. Lett. **62**, 1651 (1989).
[9]J. Peters and B. Krebs, Acta Crystallogr. B **38**, 1270 (1982).
[10]R. L. Mozzi and B. E. Warren, J. Appl. Crystallogr. **2**, 164 (1969).
[11]R. F. Pettifer, R. Dupree, I. Farnan, and U. Sternberg, J. Non-Cryst. Solids **106**, 408 (1988).
[12]R. J. Bell and P. Dean, Nature **212**, 1354 (1966); Philos. Mag. **25**, 1381 (1972).
[13]P. H. Gaskell and I. D. Tarrant, Philos. Mag. B **42**, 265 (1980).
[14]J. L. Robertson and S. C. Moss, J. Non-Cryst. Solids **106**, 330 (1988).
[15]P. N. Sen and M. F. Thorpe, Phys. Rev. B **15**, 4030 (1977); M. F. Thorpe and F. L. Galeener, *ibid.* **22**, 3078 (1980); S. W. de Leeuw and M. F. Thorpe, Phys. Rev. Lett. **55**, 2879 (1985).
[16]R. B. Laughlin and J. D. Joannopoulos, Phys. Rev. B **16**, 2942 (1977).
[17]R. A. Barrio, F. L. Galeener, and E. Martinez, Phys. Rev. Lett. **52**, 1786 (1984).
[18]A. Rahman, R. H. Fowler, and A. H. Narten, J. Chem. Phys. **57**, 3010 (1972).
[19]L. V. Woodcock, C. A. Angell, and P. Cheeseman, J. Chem. Phys. **65**, 1565 (1976).
[20]T. F. Soules, J. Chem. Phys. **71**, 4570 (1979); J. Non-Cryst. Solids **49**, 29 (1982).
[21]S. K. Mitra, M. Amini, D. Fincham, and R. W. Hockney, Philos. Mag. B **43**, 365 (1981); S. K. Mitra, *ibid.* **45**, 529 (1982).
[22]S. H. Garofalini, J. Chem. Phys. **76**, 3189 (1982).
[23]J. D. Kubicki and A. C. Lasaga, Am. Mineral. **73**, 941 (1988).
[24]B. Feuston and S. H. Garofalini, J. Chem. Phys. **89**, 5818 (1988).
[25]P. Vashishta, R. K. Kalia, J. P. Rino, and I. Ebbsjö, Phys. Rev. B **41**, 12 197 (1990).
[26]P. A. V. Johnson, A. C. Wright, and R. N. Sinclair, J. Non-Cryst. Solids **58**, 109 (1983).
[27]S. Susman *et al.*, Phys. Rev. B **43**, 1194 (1991).
[28]R. A. B. Devine, R. Dupree, I. Farnan, and J. J. Capponi, Phys. Rev. B **35**, 2560 (1987).
[29]A. C. Wright, J. Non-Cryst. Solids **106**, 1 (1988).
[30]F. L. Galeener, J. Non-Cryst. Solids **49**, 53 (1982); F. L. Galeener, R. A. Barrio, E. Martinez, and R. J. Elliott, Phys. Rev. Lett. **53**, 2429 (1984).